Chalcogenide Letters Vol. 21, No. 4, April 2024, p. 293 - 304

Structural, elastic, mechanical, and electronic properties of chalcogenide perovskite $SnZrS_3$ under pressure

S. Y. Chen[a,*], W. Wang[b]
[a]*Gannan Normal University, Ganzhou, 341000, China*
[b]*Jiangxi University of technology, Nanchang, 330098, China*

In this paper, we have presented the structural, elastic, mechanical, and electronic properties of the transition metal chalcogenide perovskite $SnZrS_3$ under different pressures by using first-principles method. Our calculated lattice parameters at ambient pressure are in good agreement with the experimental and previous theoretical results. The elastic constants were evaluated numerically for orthorhombic $SnZrS_3$ using the strain-stress approach. Orthorhombic $SnZrS_3$ shows a strong anisotropic behavior of the elastic and structural properties. According to the calculations of the electronic properties, we find the states near the valence band top are derived from S 3p, Zr 4d, Sn 5p, and Sn 5s orbitals, and the lowest conduction band is composed of Zr 4d, S 3p, and Sn 5p orbitals. As the pressure increases, the conduction and valence band shift to lower and higher energies, respectively. These results indicated that lattice constants and band gap decrease with the increase of pressure.

(Received November 15, 2023; Accepted April 1, 2024)

Keywords: Transition metal chalcopyrite perovskite, High pressure, Elastic constant, Electronic properties

1. Introduction

$SnZrS_3$ belongs to an important families of transition metal chalcogenide perovskites that have promising applications in optoelectronic industry[1-2]. Recently, transition metal chalcogenide perovskite sulfides and selenides have been successfully synthesized[3]. Its unique advantages such as high absorption coefficient values, small effective masses, and high luminescence efficiency, indicating their suitability for electronic, optical, and energy conversion technologies[4-6]. Moreover, with respect to applications, it is urgent to elucidate the structure-property relationship for expanding the recognition and continuing research.

Under ambient conditions, the structure of $SnZrS_3$ is found to be crystallized in an orthorhombic structure with space group 62/Pnma[7]. The structure is the type of NH_4CdC_{13} with edge-sharing double columns zirconium octahedral structure. It is generally accepted that the structural, elastic, mechanical, and electronic properties of materials are closely associated with their crystal structures, which can be regulated by pressure[8-9]. N. Ben Bellil *et al* have undertaken fundamental research on the structural, optoelectronic, and thermodynamics properties of the $SnZrS_3$ compound[10]. They showed that the $SnZrS_3$ conduction band minima are dominated by Zr

* Corresponding author: chenshuya202310@126.com
https://doi.org/10.15251/CL.2024.214.293

d-states, while chalcogen p-states with contributions from Sn s-states occupy the valence band maxima. Other studies also confirm that $SnMS_3$ and $SnMSe_3$ (M = Zr, Hf) materials show symmetrical doping potential as p- and n-type semiconductors which results in their suitability for homojunction photovoltaic applications[11-12]. In spite of some studies on the $SnZrS_3$, while there are few reports about the understanding of high-pressure structural details and properties. High pressure processed chalcogenide perovskite materials have obtained many exhilarating results such as photo-response enhancement, structural stability enhancement, bandgap optimization[13-14]. Pressure, as a clean tuning knob, is widely used because it can successfully modulate the electronic structure, bonding patterns and chemical behavior without changing the chemical composition[15]. Success in discovery of novel phenomena and even acquisition of new materials were obtained upon compression. In this paper, we present the structural, elastic, mechanical, and electronic properties of transition metal chalcogenide perovskite $SnZrS_3$ under different pressures using the first-principles method within density functional theory. The information of lattice parameters, band structure, total density of states (DOS) and partial density of states (PDOS) under pressure are provided. Meanwhile, the values of mechanical parameters, such as the elastic constant, and elastic moduli are also calculated. Moreover, the present study provides a good comparison between the structural and microstructural properties of chalcogenide perovskite materials. The paper is organized as follows: In Section 2, we give a brief description of the background of the theory and the details of our calculation method in this work. In Section 3, the main results of the structural, elastic, mechanical, and electronic properties of $SnZrS_3$ are presented. We draw the conclusions in Section 4.

2. Computational details

The calculations were carried out within the frame work of the density functional theory (DFT). All DFT calculations are performed using the plane-wave projector-augmented wave (PAW) method as implemented in the Vienna Ab-initio Simulation Package (VASP)[16-17]. To optimize the structure the generalized gradient approximation (GGA) functional based on Perdew-Burke-Ernzerhof (PBE) exchange-correlation functional is used[18-20]. The theoretical calculation procedures we applied consisted of the following steps: (1) establishing a reasonable crystal structure model of the $SnZrS_3$; (2) selecting calculated parameters to optimize the crystal structure at ground (0 K, 0 GPa) and high-pressure states, and then comparing the obtained lattice constants with the corresponding experimental results; (3) obtaining the final optimized crystal structures at the ground and high-pressure states that agree well with the experimental results by constantly adjusting the calculated parameters; (4) calculating the elastic and electronic properties of the final optimized crystal structures, and then analyzing the results using appropriate theories. The cut-off energy of 550 eV is used throughout the calculations. For all the structures, the total energy convergence has been tested within a tolerance level of 0.005 meV/atom[28]. The self-consistent calculations were carried out with a 6×6×10 k-point mesh. The unit cell parameters and atomic positions were optimized using the Broyden-Fletcher-Goldfarb-Shanno (BFGS) algorithm to find the lowest energy state[21]. To balance accuracy and speed, the convergence criteria for total energy, max force, max tress, and SCF iterations were $5 \times 10^{-6}\mathrm{eV/atom}$, $0.01\mathrm{eV/Å}$, 0.02 GPa, and $5 \times 10^{-7}\mathrm{eV/atom}$, respectively.

3. Results and discussion

3.1. Structural properties

In order to know the reliability of our parameters, it is obligatory to calculate the values of equilibrium lattice parameters (*a*, *b*, and *c*) and volume of $SnZrS_3$ before studying the pressure dependence of mechanical and electronic properties. Lattice parameters and the volume at zero pressure are summarized in Table 1, together with experimental[7] and other theoretical data for comparison[10]. Based on the GGA functional, the calculated optimized lattice parameters of orthorhombic $SnZrS_3$ at zero pressure is *a*=9.345 Å, *b*=3.743 Å, *c*=13.688 Å, and the previously obtained experimental values are *a*=9.188 Å, *b*=3.717 Å, *c*=13.839 Å. The comparison shows that our results are very close to the available data, and the present values *a*, *b*, and *c* deviate from experimental values within 3%, which ensure the reliability of our DFT based investigation.

Table. 1. The calculated equilibrium structural parameters of orthorhombic $SnZrS_3$ at ambient pressure. The previous experimental results are also listed.

Method	a_0 (Å)		b_0(Å)	c_0(Å)
V(Å^3)				
GGA	9.345	3.743	13.688	478.87
LDA	9.105	3.669	13.261	443.09
[10]Cal.	9.123	3.722	13.790	468.25
[7]Expt.	9.183	3.719	13.829	472.63

Additionally, in order to evaluate the influence of pressure effect on the structure parameters, the equilibrium geometries of orthorhombic $SnZrS_3$ were computed at fixed values of applied hydrostatic pressure in the range from 0 to 10 GPa with a step of 1 GPa. The relative lattice parameters and relative cell volumes curves as functions of the pressure up to 10 GPa are plotted in Fig. 1. It manifests that when the pressure increases, the lattice constants *a*, *b*, and *c* decrease, and the volume of the unit cell becomes small. As the pressure increases from 0 to 10 GPa, the lattice parameter along the *a*-axis decreases from 9.345 to 8.509 Å. The value of the lattice constant *b* is reduced by 0.692 Å with increase of the external pressure from 0 to 10 GPa, while *c* shows a pressure dependence of $\Delta c = 0.364$ Å, respectively. It can be clearly seen that the lattice parameter *a* decrease slightly faster than the other lattice parameters *b*, and *c*. From a theoretical point of view, as the pressure increases, the interaction of Sn, Zr, and S atoms becomes stronger and therefore the bond length among these atoms becomes shorter as a result the lattice parameters become smaller with pressure[22]. Moreover, fitting lattice parameters *a*, *b*, and *c* to linear equation dependent on pressure give the following relationships: $a(P)=9.302-0.082P$; $b(P)=3.737-0.014P$; $c(P)=13.579-0.065P$. The slope of fitting linear equation of lattice parameters *a*, *b* and *c* are -0.082 Å/GPa, -0.014 Å/GPa and -0.065 Å/GPa, respectively. It suggests that the lattice parameter *a* is more sensitive to external pressure than *b* and *c*. This indicates that the crystal structure of orthorhombic $SnZrS_3$ is continuously compressed with increases in pressure is the most compressible along the *a*-axis and stiffest along the *b*- and *c*-axis. This can attribute to the

bonding of Sn-S and Zr-S layers along the *b*-axis and *c*-axis are stronger than the interlayer interactions along the *a*-axis. Therefore, the lattice parameter along the *a*-axis is more sensitive to pressure than that along the other *b*-axis and *c*-axis. The non-uniform pressure dependence of the lattice parameters may also mean that the orthorhombic $SnZrS_3$ undergoes anisotropic compression.

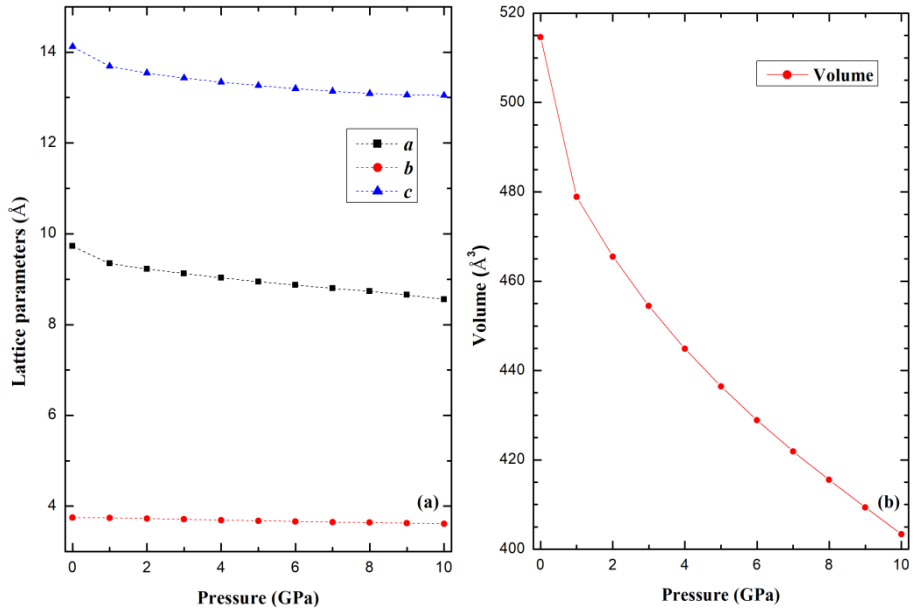

Fig. 1. The lattice parameters and cell volume of the orthorhombic $SnZrS_3$ as a function of pressure.

Meanwhile, the obtained pressure-unit cell volume (*P-V*) data set was used to obtain the Bulk modulus B_0 and its pressure derivative B_0' by fitting the data to the Birch-Murnaghan equation of state (EOS)[23] (Fig. 1(b)) along with the experimental data. At 10 GPa, the volume compression is $V/V_0 = 83.15\%$, ($V = 398.16$ Å^3, $V_0 = 478.87$ Å^3). The pressure derivative of bulk modulus is a parameter of great physical significant in high pressure physics. The obtained parameters for the bulk modulus and its first pressure derivative at ambient pressure and temperature is $B_0 = 82.32\ GPa$ GPa and its derivative is B_0'=4.17, respectively, which are found to yield similar results in the pressure range for the theoretical data of $B_0 = 81.412\ GPa$ and $B_0' = 4.139$ [10]. These results are expected to provide useful guidance for the structural characterization of this material under high pressure.

3.2. Elastic properties and mechanical stability

Elastic constants are important mechanical parameters of solid materials, which determine the stiffness of a crystal against the external strain[24-26]. Thus, we calculate the elastic constants to study the mechanical properties of chalcogenide perovskite materials under different pressures. Secondly, the elastic constant describe the stability of the structure, anisotropy, brittle, and ductile behavior. For an orthorhombic structure, $SnZrS_3$ has nine independent elastic constants which are summarized in Table 2 with available theoretical data. All the calculated elastic constants agree

well with the previous theoretical results. Unfortunately, there are no available experimental data to compare with our results. For orthorhombic crystal, the mechanical stability requires the elastic constants satisfying the well-known Born stability criteria[27]: $C_{11}+C_{22}-2C_{12}>0$; $C_{11}+C_{33}-2C_{13}>0$; $C_{33}+C_{22}-2C_{23}>0$ and $(C_{11}+C_{22}+C_{33}+2C_{12}+2C_{13}+2C_{21})>0$ and $C_{ii}>0$. It is found that our calculated elastic constants can meet the mechanical stability conditions mentioned above, which indicates that it is mechanically stable over the pressure range of 0 to 10 GPa.

Table. 2. The calculated elastic constants of the orthorhombic $SnZrS_3$ under zero pressure together with other theoretical values[23].

Pressure	C_{11}	C_{22}	C_{33}	C_{44}	C_{55}	C_{66}	C_{12}	C_{13}	C_{23}
0 GPa	24.5	91.3	22.9	6.3	9.1	16.2	10.7	10.2	2.9
2 GPa	50.7	109.1	60.4	16.9	19.9	32.4	26.4	29.1	18.9
4 GPa	64.2	119.5	83.5	19.7	26.2	40.2	35.2	40.1	25.5
6 GPa	73.3	127.8	102.2	25.3	29.7	45.8	42.7	48.6	31.8
8 GPa	82.9	135.7	114.6	26.4	33.6	51.3	45.5	63.3	34.9
10 GPa	87.3	142.3	135.5	31.6	38.1	57.6	55.6	47.9	39.4

The elastic constants of the orthorhombic $SnZrS_3$ under different pressures are shown in Fig. 2. It was found that the elastic constants slightly increased with the increasing pressure up to 10 GPa. However, the elastic constants C_{44} and C_{55} have little change with the increasing pressure. The elastic constants C_{11}, C_{22}, and C_{33} are related to the deformation behavior and atomic bonding characteristics. The elastic constants C_{11}, C_{22}, and C_{33} represent the resistance to linear compression (direction of the applied force) and the other elastic constants C_{12}, C_{13}, C_{23}, C_{44}, C_{55}, and C_{66} are mainly associated with the elasticity in shape (shear stress). In the entire pressure range of our calculation, C_{11}, C_{22}, and C_{33} were much larger than those of the other elastic constants, indicating that deformation resistances along the axial direction were stronger than the deformation resistances in shape. Furthermore, it can be seen from Figure. 2 that the relationship of the resistance to linear compression $C_{22}>C_{33}>C_{11}$ for orthorhombic $SnZrS_3$. This indicates the weaker resistance to the unidirectional compression compared to the resistance to shear deformation. These results are consistent with the results in Figure. 1 showing that with increased pressure, the lattice parameter *a* decreased faster than lattice parameters *b* and *c*. To the best of our knowledge, there are currently no available experimental data about the elastic constants of orthorhombic $SnZrS_3$ for our comparison. We consider the present results of elastic constants as a prediction study hoping that our present work will stimulate some more works on these materials.

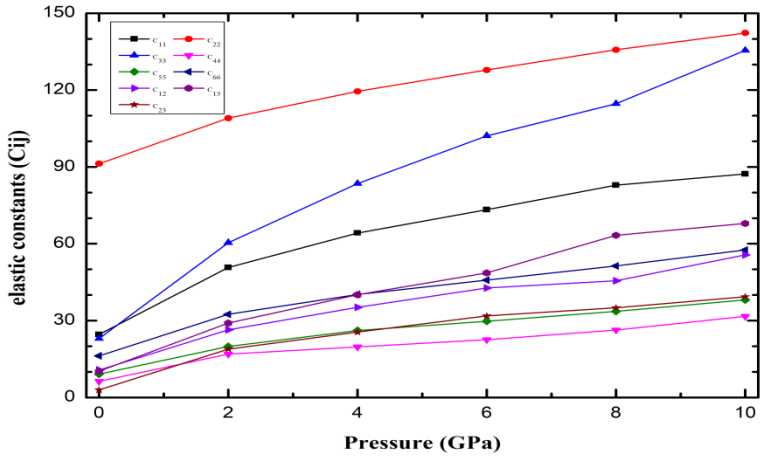

Fig. 2. The elastic constants of the orthorhombic $SnZrS_3$ as functions of pressures.

Meanwhile, the bulk modulus (B) reflects the resistance of materials against volume change. The shear modulus (G) reflects the resistance of materials against shape change. The Young's modulus (E) measures the stiffness of materials[28]. To further investigate the influence of pressure on the mechanical properties, based on the elastic constants, we calculated the bulk modulus, shear modulus, and Young's modulus of orthorhombic $SnZrS_3$ at different pressures by using the Voigt-Reuss-Hill approximations method[29-31]. On the basis of Voigt approximation, the shear modulus (G_V) and bulk modulus (B_V) as the function of elastic constants (C_{ij}) are given as: $B_V = \frac{1}{9}[C_{11} + C_{12} + C_{33} + 2(C_{12} + C_{13} + C_{23})]$; $G_C = \frac{1}{15}[C_{11} + C_{22} + C_{33} + 3(C_{44} + C_{55} + C_{66}) - (C_{12} + C_{13} + C_{23})]$. On the basis of Reuss approximation, the shear modulus (G_R) and bulk modulus (B_R) can be defined as follows: $B_R = 1/(s_{11} + s_{22} + s_{33}) + 2(s_{12} + s_{13} + s_{23})$; $G_R = 15/[4(s_{11} + s_{22} + s_{33}) - 4(s_{12} + s_{13} + s_{23}) + 3(s_{44} + s_{55} + s_{66})]$. Since these approximations from Voigt and Reuss are upper and lower bounds of elastic constants, respectively. Therefore, Hill's averages are used to predict bulk modulus (B) and shear moduli (G) of the polycrystalline aggregates by: $B=1/2(B_R + B_V)$; $G=1/2(G_R + G_V)$. The Young's modulus (E) and Poisson's ratio (δ) are given by the following formulas: $E=9BG/(3B+G)$; $\delta=(3B-2G)/(2(3B+G))$. The variation curves of the bulk modulus, Young's modulus and shear modulus with regard to the applied pressure are exhibited in Fig. 3. It is found that the bulk modulus B, shear modulus G, and Young's modulus E increase with pressure, suggesting that the orthorhombic $SnZrS_3$ is more difficult to compress as pressure increases. As can be seen, the value of bulk modulus B and shear modulus E at 10 GPa is 4.86 and 2.92 times greater than that at 0 GPa, respectively. Additionally, B is larger than G, indicating the parameter limiting stability of the compound is shear modulus. Moreover, the brittle and ductility nature of the orthorhombic $SnZrS_3$ are analyzed according to the Pugh's ratio (B/G), and Poisson's ratio (δ). A material with a B/G ratio value less than 1.75 is associated with brittle nature. Otherwise, materials should have ductility[28]. The ductility and brittleness of materials are also separated by the Poisson's ratio with the critical value of 0.26. If the Poisson's ratio is less than 0.26, then brittle behavior is predicted; otherwise, materials should behave in a ductile manner[32-33]. From figure. 3 (b), the value of B/G for orthorhombic $SnZrS_3$ at 0 GPa is about 0.95. And with the increasing pressure, the value of B/G becomes more and more

greater. In our calculations, when the pressure up to 10 GPa, the value of B/G is about 2.07, implying pressure can improve the ductility of orthorhombic $SnZrS_3$. From figure. 3 (c), our results show that the Poisson's ratios change from 0.131 (P = 0 GPa) to 0.295 (P = 10 GPa) which are larger than 0.26. With the increase of pressure, our calculated Poisson's ratios increases gradually. When the pressure is more than 4 GPa, Poisson's ratios are more than 0.26 and orthorhombic $SnZrS_3$ shows ductility, which is consistent with the results of the Pugh's criterion. These results show that orthorhombic $SnZrS_3$ changes from brittleness to ductility with the increase of pressure.

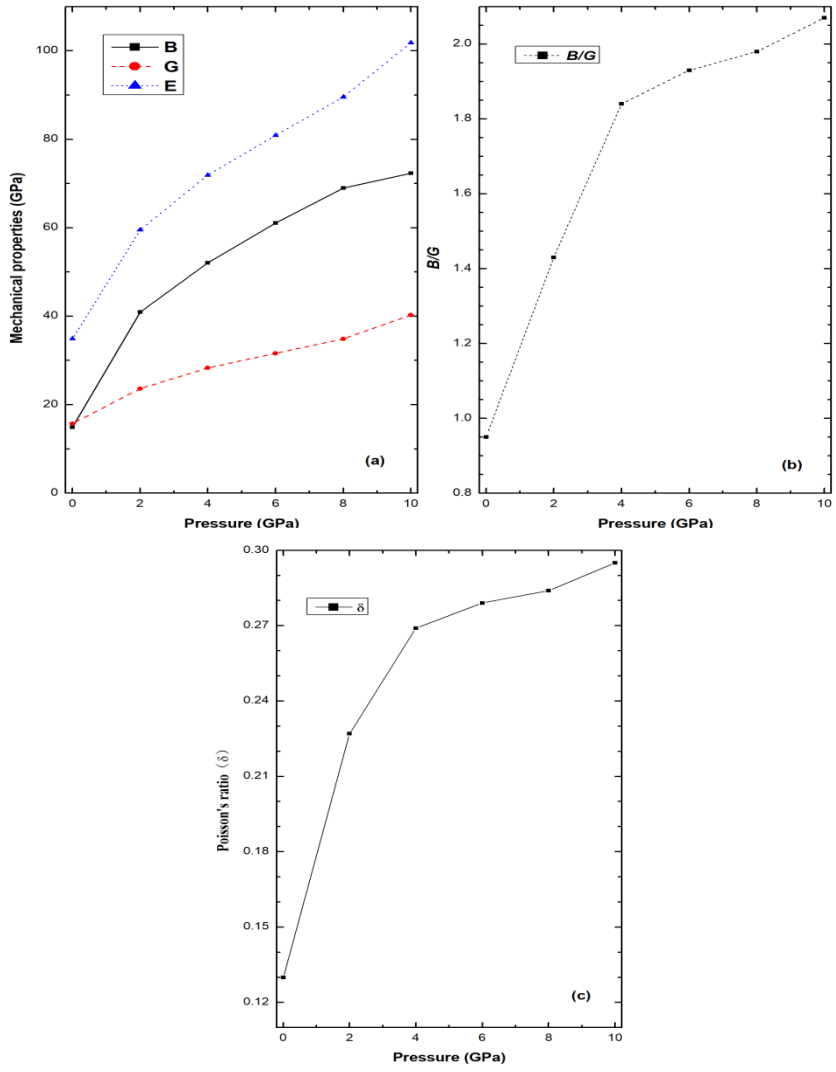

Fig. 3. The pressure dependence of (a) elastic moduli B, G, and E (b) Poisson's ratio, and (c) the quotient of shear to bulk modulus for orthorhombic $SnZrS_3$.

3.3. Electronic structure and density of state

For the equilibrium geometry of the orthorhombic $SnZrS_3$, electronic structures such as band structure, the total density of states (DOS) and the density of partial states (PDOS) have been calculated by first-principles based on the density function theory. To gain more knowledge about

physical characteristics of orthorhombic $SnZrS_3$ compound, the energy band structures were calculated along with specials lines connecting the high symmetry points in the first Brillouin zone. The internal coordinates of these highest symmetry points G, Z, T, Y, S, X, U, and R are (0, 0, 0), (0, 0, 0.5), (-0.5, 0, 0.5), (-0.5, 0, 0), (-0.5, 0.5, 0), (0, 0.5, 0), (0, 0.5, 0.5) and (-0.5, 0.5, 0.5) in the first Brillouin zone, respectively. The calculated energy band structure along the high symmetry directions in the first Brillouin zone of orthorhombic $SnZrS_3$ the using the GGA+PBE functional at ambient pressure and 10 GPa are shown in Fig. 4. From the figure, it is seen that at zero pressure the top of the valence band (VB) is at T symmetry point, while the bottom of the conduction band (CB) is located at G point. The calculated band gap of the material at zero pressure (1.14 eV) is similar to most theoretical calculations[34]. And we found that our computed results of the bandgap values at the level of the GGA+PBE approach are in nice agreement with the available experimental result of 1.18 eV. From the plot of the band structure, one can see that orthorhombic $SnZrS_3$ at zero pressure is an indirect bandgap semiconductor. A similar band gap nature for the compound at zero pressure is also reported by a recent work of N. B. Bellil *et al*, which confirms our results[10]. Interestingly, when we increase pressure, the top of the VB at T shifts to the Fermi level, while it shifts away from the Fermi level at G symmetry point; transforming the material to a direct band gap (G-G) at the pressure up to 10 GPa. The conversion from indirect to direct band gap of chalcogenide perovskite compounds with pressure predicts some interesting theoretical results, which shows its effectiveness in high frequency optoelectronic devices applications[34-35].

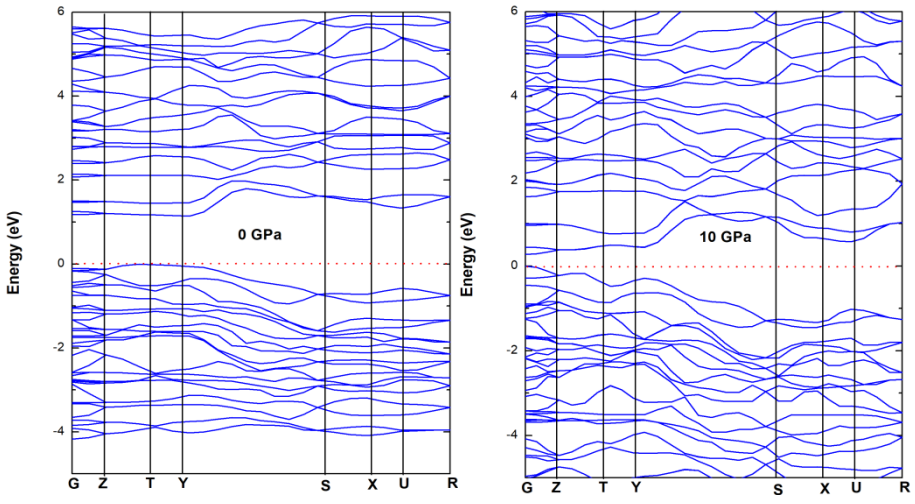

Fig. 4. The band structures of the orthorhombic SnZrS3 at 0 GPa, and 10 GPa, respectively. The red dashed line is marked the Fermi level.

Moreover, the total and partial density of states provide more details about the electronic properties of atoms and orbitals. To further elucidate the nature of the electronic band structure, the total density of states (DOS) and partial density of states (PDOS) of orthorhombic $SnZrS_3$ under 0 GPa, and 10 GPa are shown in Fig. 5. The states near the valence band top are derived from S 3p, Zr 4d, Sn 5p, and Sn 5s orbitals, and the lowest conduction band is composed of Zr 4d, S 3p, and Sn 5p orbitals. These results agree with the previous calculation results[36]. However, as the pressure increases, the conduction and valence band shift to lower and higher energies, respectively. This

energy shift results in the decrease of band gap substantially, which are in agreement with band structures and explain the band structures as well. The reason for this is likely to be that the distance between the atoms decreases under the effect of high pressure, which leads to a change in the atomic orbitals occupied by electrons, which results in the appearance of new hybridizations between different elements. The pressure dependence of the band gap is shown in Fig. 6, clearly indicating the band gap decrease with increasing pressure. To determine the pressure coefficient, we fitted the direct band gap to determine the pressure coefficient, we fitted the direct band gap ($E_g(P)$) with a quadratic function: $E_g(P)=Eg(0)+aP+bP^2$, and obtained a=-0.107 eV/GPa and b=0.002 eV/(GPa)^2.

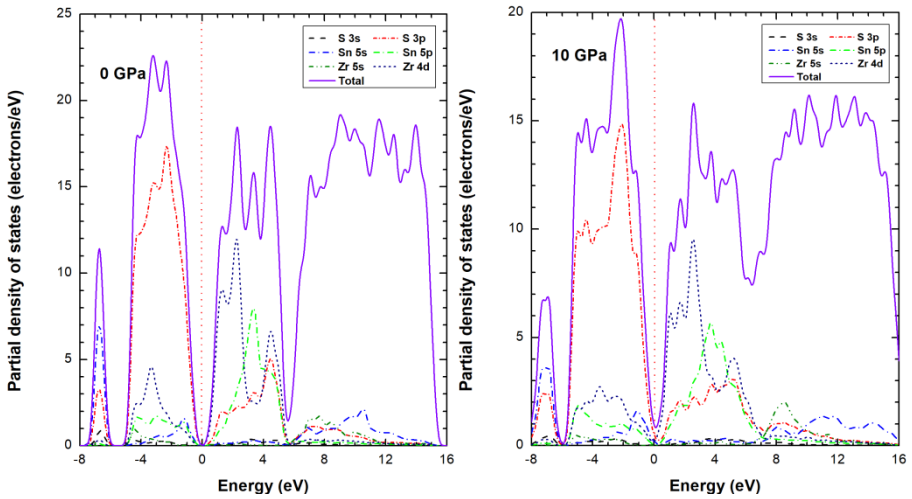

Fig. 5. The density of state (DOS) and partial density of state (PDOS) of the orthorhombic $SnZrS_3$ at 0 GPa, and 10 GPa, respectively. The red dashed line is marked the Fermi level.

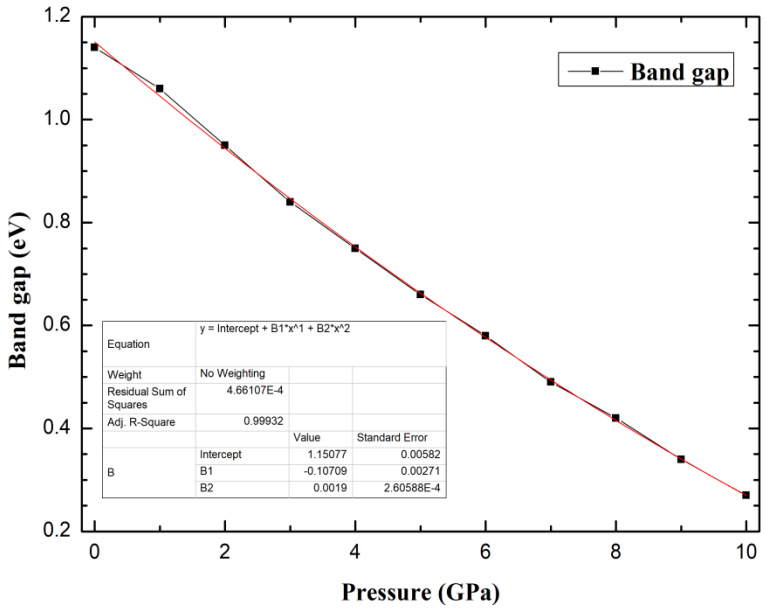

Fig. 6. The pressure variations of energy band gaps for orthorhombic $SnZrS_3$.

4. Conclusion

Structural parameters, mechanical, and electronic properties of orthorhombic $SnZrS_3$ have been investigated up to 10 GPa, based on the first-principles density functional theory. It is found that at zero pressure, the structural parameters are in good agreement with the experimental results. By increasing pressure; the lattice constant as well as cell volume decrease with the increasing pressure. The single crystal elastic constants of the orthorhombic $SnZrS_3$ increased with increasing pressure match the Born stability criteria. The polycrystalline elastic modulus exhibit a monotonous behavior under pressure. According to Pugh's criterion and Poisson's ratio, it is found that the transition from the brittle to ductile material and the mechanical properties exhibit a monotonous behavior under pressure. Meanwhile, the pressure dependence of the electronic band structure, density of states and partial density of states of orthorhombic $SnZrS_3$ were presented. The compound exhibits indirect band gap nature at zero pressure, while by increasing pressure the band gap shifts from indirect to direct. According to our work, we found that the band gap decreases with the pressure, which provide some additional information about these chalcopyrite semiconductors under pressure to fundamental material physics.

Acknowledgments

This work was supported by Jiangxi Provincial Education Planning Project (group no：20YB171).

References

[1] J. W. Bennett, I. Grinberg, A. M. Rappe, Phys. Rev. B 79 (2009) 235115; https://doi.org/10.1103/PhysRevB.79.235115

[2] Niu, H. Huyan, Y. Liu, M. Yeung, K. Ye, L. Blankemeier, T. Orvis, D. Sarkar, D. J. Singh, R. Kapadia, J. Ravichandran, Adv. Mater. 29 (2017) 1604733; https://doi.org/10.1002/adma.201604733

[3] Meng, B. Saparov, F. Hong, J. Wang, D. B. Mitzi, Y. Yan, Chem. Mater. 28 (2016) 821; https://doi.org/10.1021/acs.chemmater.5b04213

[4] M. Brik, M. Piasecki, I. Kityk, Inorg. Chem. 53 (2014) 26451; https://doi.org/10.1021/ic500200a

[5] H. Reshak, Z. A. Alahmed, J. Bila, V. Victor, G. Atuchin, O. D. Bazarov, J. Phys. Chem. C 120 (2016)10559; https://doi.org/10.1021/acs.jpcc.6b01489

[6] P. Hohenberg, W. Kohn, Phys. Rev. 136 (1964) B864; https://doi.org/10.1103/PhysRev.136.B864

[7] A. Meetsma, G. A. Wiegers, J. L. de Boer, Acta. Cryst. C 49 (1993) 2060; https://doi.org/10.1107/S0108270193005888

[8] G. K. H. Madsen, P. Blaha, K. Schwarz, E. Sjostedt, L. Nordstrom, Phys. Rev. B 64, (2001) 195134; https://doi.org/10.1103/PhysRevB.64.195134

[9] K. Schwarz, P. Blaha, G. K. H. Madsen, Comput. Phys. Commun. 147 (2002) 71; https://doi.org/10.1016/S0010-4655(02)00206-0

[10] N. Ben Bellil, F. Litimein, H. Khachai, R. Khenata, A. Abdiche, E. Güler, R. Ahmed, A. Bouhemadou, S. B. Omran, J. M. Khalifeh, Mater. Today Commun. 27 (2021) 102427; https://doi.org/10.1016/j.mtcomm.2021.102427

[11] G. A. Wiegers, A. Meetsma, R. J. Haange, J. L. de Boer, Solid State Ion. 32 (1989) 183; https://doi.org/10.1016/0167-2738(89)90220-8

[12] H. Nishiate, K. Suekuni, J. Appl. Phys. 125 (2019) 175111; https://doi.org/10.1063/1.5093183

[13] C. Persson, J. Appl. Phys. 107 (2010) 053710; https://doi.org/10.1063/1.3318468

[14] Z. Y. Zhao, C. S. Ma, Y. C. Cao, J. Yi, X. J. He and J. B. Qiu, Phys. Lett. A377 (2013) 417. 15D. Amgar, A. Stern, D. Rotem, D. Porath, L. Etgar, Nano Lett. 17 (2017) 1007; https://doi.org/10.1021/acs.nanolett.6b04381

[16] D.Vanderbilt, Phys. Rev. B 41 (1990) 7892; https://doi.org/10.1103/PhysRevB.41.7892

[17] G. Kresse, J. Hafner, Phys. Rev. B 47 (1993) 558; https://doi.org/10.1103/PhysRevB.47.558

[18] M. Ceperley, B. J. Alder, Phys. Rev. Lett. 45 (1980) 566; https://doi.org/10.1103/PhysRevLett.45.566

[19] J. P. Perdew, A. Zunger, Phys. Rev. B 23 (1981) 5048; https://doi.org/10.1103/PhysRevB.23.5048

[20] J. P. Perdew, K. Burke, M. Ernzerhof, Phys. Rev. Lett. 77 (1996) 3865; https://doi.org/10.1103/PhysRevLett.77.3865

[21] J. D. Pack, and H.J. Monkhorst, Phys. Rev. B. 16 (1977) 1748; https://doi.org/10.1103/PhysRevB.16.1748

[22] H. Rozale, B. Bouhafs, P. Ruterana, Superlattice. Microst. 42 (2007) 165; https://doi.org/10.1016/j.spmi.2007.04.007

[23] B. Francis. Phys. Rev. 71 (1947) 809; https://doi.org/10.1103/PhysRev.71.809

[24] F. Tran, P. Blaha, Phys. Rev. Lett. 102 (2009) 226401; https://doi.org/10.1103/PhysRevLett.102.226401

[25] C. Stampfl, C. G. Van de Walle, Phys. Rev. B 59 (1999) 5521; https://doi.org/10.1103/PhysRevB.59.5521

[26] L. J. Sham, M. Schlüter, Phys. Rev. Lett. 51 (1983) 1888; https://doi.org/10.1103/PhysRevLett.51.1888

[27] F. Mouhat. and F. X. Coudert. Phys. Rev. B. 90 (2014) 224104; https://doi.org/10.1103/PhysRevB.90.224104

[28] I. R. Shein, A. L. Ivanovskii, J. Phys. Condens. Mater. 20 (2008) 415218; https://doi.org/10.1088/0953-8984/20/41/415218

[29] Z. Wu, E. Zhao, H. Xiang, X. Hao, X. Liu, J. Meng, Phys. Rev. B 76 (2007) 054115; https://doi.org/10.1103/PhysRevB.76.054115

[30] J. I. Tani, M. Takahashi, H. Kido, Comp. Mater. Sci. 50 (2011) 2009; https://doi.org/10.1016/j.commatsci.2011.01.053

[31] M. Mattesini, S. F. Matar, Phys. Rev. B 65 (2002) 075110; https://doi.org/10.1103/PhysRevB.65.075110

[32] P. Ravindran, LarsFast, P. A. Korzhavyi, B. Johansson, J. Wills, O. Eriksson, J. Appl. Phys. 84 (1998) 4891; https://doi.org/10.1063/1.368733

[33] S. F. Pugh, Philos. Mag.7 (1954) 823; https://doi.org/10.1080/14786440808520496

[34] F. Tran, P. Blaha, Phys. Rev. Lett. 102 (2009) 226401; https://doi.org/10.1103/PhysRevLett.102.226401

[35] S. V. Borisov, A. Magarill, V. Pervukhin. J. Struct. Chem. 57 (2016) 512; https://doi.org/10.1134/S0022476616030136

[36] O. V. Parasyuk, O. Y. Khyzhun, M. Piasecki, I. V. Kityk, P. M. Fochuk, Mater. Chem. Phys. 187 (2017) 156; https://doi.org/10.1016/j.matchemphys.2016.11.061